PHYSICAL REVIEW D **91,** 125034 (2015)

Effective model for the QCD phase transitions at finite baryon density

S. Benić,[1,2] I. Mishustin,[3,4] and C. Sasaki[3,5]

[1]*Physics Department, Faculty of Science, University of Zagreb, Zagreb 10000, Croatia*
[2]*Department of Physics, The University of Tokyo, 7-3-1 Hongo, Bunkyo-ku, Tokyo 113-0033, Japan*
[3]*Frankfurt Institute for Advanced Studies, D-60438 Frankfurt am Main, Germany*
[4]*Kurchatov Institute, Russian Research Center, Akademika Kurchatova Square, Moscow 123182, Russia*
[5]*Institute of Theoretical Physics, University of Wrocław, PL-50204 Wrocław, Poland*

(Received 26 February 2015; published 26 June 2015)

We introduce an effective quark-meson-nucleon model for the QCD phase transitions at finite baryon density. The nucleon and the quark degrees of freedom are described within a unified framework of a chiral linear sigma model. The deconfinement transition is modeled through a simple modification of the distribution functions of nucleons and quarks, where an additional auxiliary field, the bag field, is introduced. The bag field plays a key role in converting between the nucleon and the quark degrees of freedom. The model predicts that the chiral and the deconfinement phase transitions are always separated. Depending on the model parameters, the chiral transition occurs in the baryon density range of $(1.5-15.5)n_0$, while the deconfinement transition occurs above $5n_0$, where n_0 is the saturation density.

DOI: 10.1103/PhysRevD.91.125034 PACS numbers: 12.39.Fe, 12.38.Mh, 25.75.Nq

I. INTRODUCTION

The basic problem of QCD thermodynamics is to understand the conversion from hadrons to quarks and gluons and how this is related to the underlying chiral and deconfinement transitions. This problem has major relevance to the physics of heavy ion collisions and compact stars [1–4]. At present there are several proposals to effectively convert between the hadronic and the quark-gluon phase, with partial success. At finite T, quark degrees of freedom can be suppressed by the Polyakov loop [5–7]. Mechanisms for excluding composite degrees of freedom are the spectral function method [8–13] and the excluded volume method, for recent works see Refs. [14–17].

In this work we construct an effective quark-meson-nucleon model with two flavors for the QCD phase transitions at finite density. We place several restrictions on our approach: first we must take into account both the nuclear and the quark degrees of freedom. Second, the model should respect global symmetries of QCD, i.e. the chiral symmetry and the scale invariance. Third, quark degrees of freedom must be excluded at the nuclear matter density, and nuclear degrees of freedom must be excluded at some high density. We require that the model reproduces the nuclear matter ground state. Finally, a unified description must encompass couplings of nucleons and quarks to the same bosonic mean-fields generated from a unique vacuum potential.

For nucleons, both chiral and scale invariance can be accommodated in the parity doublet model [18–24] [25–27]. The quark sector is described by a linear sigma model [28,29] coupled to the dilaton [30]. We find that the small σ mass as required for reasonable nuclear matter properties [21] results in a shallow potential in the σ direction. As an immediate consequence, pure quark matter appears at baryon chemical potentials μ_B below the value of the vacuum nuclear mass. In order to solve this problem we generalize the idea of statistical confinement from effective model studies at finite T to finite densities. While at finite T the Polyakov loop is used to statistically suppress thermal quark fluctuations [5], its extension to finite baryon chemical potential is problematic. In this work we use instead the concept of infrared confinement [31,32] in order to modify the Fermi-Dirac distributions of quarks. We consider a simple model where the Fermi distribution of quarks is restricted to momenta above b, where b is a new auxiliary field in our model, which we name the *bag* field. The finite value of b in the vacuum and at low temperatures and densities is guaranteed by a new phenomenological vacuum potential. We fit the parameters of this potential to the QCD vacuum energy and by matching the pseudocritical temperature for the chiral and deconfinement transition known from the lattice simulations at $N_f = 2$ [33,34]. The model is compared to a Polyakov-quark-meson model by pointing out their similarities and differences.

Next, we introduce a generalization of the distribution functions for the nucleons in such a way that their Fermi surface is restricted only to low momenta [32], i.e. below some value αb, where α is a new parameter. This leads to a construction of a combined quark-meson-nucleon model. We find that the minimization of the thermodynamic potential in the b field acts to convert the nucleons to quarks as the baryon chemical potential is increased. One of the main consequences of this model is that the chiral and the deconfinement transitions at $T = 0$ are *separated*.

This paper is organized as follows. In Sec. II we introduce the nucleonic model and briefly consider the nuclear matter ground state. Section III is devoted to the

quark degrees of freedom. Here we introduce the b-field potential and discuss statistical confinement of quarks. Section IV describes a combined quark-meson-nucleon model. The main results of this paper are given in Sec. V, while in the following Sec. VI we make our conclusions. In the Appendix we solve a simplified version of the quark-meson-nucleon model.

II. NUCLEONIC SECTOR: PARITY DOUBLET MODEL WITH DILATON

We consider the $N_f = 2$ nuclear parity doublet model within the mirror assignment of chiral symmetry [18–24] [25–27]. We prefer to use a linear realization of the chiral symmetry which allows the description of chiral symmetry restoration. The restoration of chiral symmetry in QCD dictates that hadrons of opposite parity become degenerate, but not necessarily massless. A finite chirally invariant mass is then modeled by a parity doublet model with mirror assignment. Note that the possibility of a chirally invariant contribution to the nucleon mass was recently hinted by lattice calculations [35]. First lattice QCD simulations of nucleon parity partners at finite T [36] find that their masses become degenerate by crossing the QCD phase transition.

The nucleonic part of the model Lagrangian [21,22] coupled to the dilaton [25–27] is

$$\begin{aligned}\mathcal{L}_N &= i\bar{\Psi}_1\partial\!\!\!/\Psi_1 + i\bar{\Psi}_2\partial\!\!\!/\Psi_2 + g_\chi\chi(\bar{\Psi}_1\gamma_5\Psi_2 - \bar{\Psi}_2\gamma_5\Psi_1)\\ &\quad + g_1\bar{\Psi}_1(\sigma + i\gamma_5\boldsymbol{\tau}\cdot\boldsymbol{\pi})\Psi_1 + g_2\bar{\Psi}_2(\sigma - i\gamma_5\boldsymbol{\tau}\cdot\boldsymbol{\pi})\Psi_2\\ &\quad - g_\omega\bar{\Psi}_1\omega\!\!\!/\Psi_1 - g_\omega\bar{\Psi}_2\omega\!\!\!/\Psi_2, \end{aligned} \tag{1}$$

where $\Psi_{1,2}$ are the nuclear chiral partners. The fermions $\Psi_{1,2}$ are coupled to the chiral fields $(\sigma, \boldsymbol{\pi})$, to the ω_μ field and to the dilaton χ. The mass eigenstates are given as

$$\begin{pmatrix} N_+ \\ N_- \end{pmatrix} = \frac{1}{\sqrt{2\cosh\delta}} \begin{pmatrix} e^{\delta/2} & \gamma_5 e^{-\delta/2} \\ \gamma_5 e^{-\delta/2} & -e^{\delta/2} \end{pmatrix} \begin{pmatrix} \Psi_1 \\ \Psi_2 \end{pmatrix}, \tag{2}$$

where

$$\sinh\delta = -\frac{g_1 + g_2}{2g_\chi}\frac{\sigma}{\chi},$$

with masses

$$m_{N_\pm} = \frac{1}{2}\left[\sqrt{(g_1+g_2)^2\sigma^2 + 4g_\chi^2\chi^2} \mp (g_1 - g_2)\sigma\right]. \tag{3}$$

The state N_+ is the nucleon $N(938)$ while N_- is its parity partner conventionally identified with $N(1500)$. The meson contribution is as follows:

$$\begin{aligned}\mathcal{L}_M &= \frac{1}{2}(\partial_\mu\sigma)^2 + \frac{1}{2}(\partial_\mu\boldsymbol{\pi})^2 + \frac{1}{2}(\partial_\mu\chi)^2 - \frac{1}{4}(\omega_{\mu\nu})^2\\ &\quad - V_\sigma - V_\omega - V_\chi, \end{aligned} \tag{4}$$

where

$$V_\sigma = \frac{\lambda}{4}\left(\sigma^2 + \boldsymbol{\pi}^2 - \frac{\lambda_\chi}{\lambda}\chi^2\right)^2 - \epsilon\sigma\chi^2, \tag{5}$$

$$V_\omega = -\frac{\lambda_\omega}{2}\chi^2\omega_\mu^2, \tag{6}$$

and

$$V_\chi = \frac{B}{4}\left(\frac{\chi}{\chi_0}\right)^4\left[\log\left(\frac{\chi}{\chi_0}\right)^4 - 1\right]. \tag{7}$$

The total Lagrangian $\mathcal{L}_N + \mathcal{L}_M$ is chiral and scale invariant. All the masses in the model are generated by the condensation of the dilaton field in the vacuum χ_0. We can fix λ_ω by $m_\omega^2 = \lambda_\omega\chi_0^2$, where $m_\omega = 783$ MeV. The parameters λ, λ_χ and ϵ are related to the sigma and pion masses and the pion decay constant f_π as

$$\lambda = \frac{m_\sigma^2 - m_\pi^2}{2f_\pi^2}, \qquad \lambda_\chi = \frac{m_\sigma^2 - 3m_\pi^2}{2\chi_0^2}, \qquad \epsilon = \frac{m_\pi^2 f_\pi}{\chi_0^2}, \tag{8}$$

with $m_\pi = 138$ MeV and $f_\pi = 93$ MeV. We take $m_+ = 938$ MeV, $m_- = 1500$ MeV [21]. The nuclear matter ground state can be obtained by fixing the parameters m_σ, g_1, g_2, g_χ, g_ω. The dilaton potential V_χ is fixed by identifying the lowest glueball mass with the dilaton mass $m_\chi = 1700$ MeV [37,38], and by fixing the value of the gluon condensate. The conventional value of the gluon condensate $\langle\frac{\alpha_s}{\pi}G_{\mu\nu}G^{\mu\nu}\rangle \simeq (331\text{ MeV})^4$ [39] is accompanied by large uncertainties, $\langle\frac{\alpha_s}{\pi}G_{\mu\nu}G^{\mu\nu}\rangle \simeq (300 - 600\text{ MeV})^4$. For recent accounts see [40–42] and references therein. By the relation for the trace anomaly this can be translated into the following range for the QCD vacuum energy $\epsilon_{\rm vac} \simeq (193 - 386\text{ MeV})^4$. Assuming that the QCD vacuum energy is dominated by the dilaton potential, the gluonic bag constant is estimated to $B \simeq (273 - 546\text{ MeV})^4$. From the relation for the dilaton mass

$$m_\chi^2 = \frac{\partial^2 V_\chi}{\partial\chi^2} = \frac{4B}{\chi_0^2}, \tag{9}$$

we obtain $\chi_0 \simeq 87.79 - 351.17$ MeV.

Since the dilaton is heavy $m_\chi = 1700$ MeV, it practically does not influence the nuclear ground state and we can adopt the model parameters from [21]. This fixes $m_\sigma = 370.63$ MeV, $g_1 = 13.00$, $g_2 = 6.97$, $g_\chi = 4.39$ and $g_\omega = 6.79$. The corresponding thermodynamic potential in the mean-field approximation is

$$\Omega = V_\sigma + V_\omega + V_\chi + \sum_{X=N_\pm} \Omega_X, \tag{10}$$

$$\Omega_X = \gamma_N \int \frac{d^3p}{(2\pi)^3} [T \log(1 - f_X) + T \log(1 - \bar{f}_X)], \tag{11}$$

where the functions f_X are the Fermi-Dirac distributions

$$f_X = \frac{1}{1 + e^{\beta(E_X - \mu_N)}}, \qquad \bar{f}_X = \frac{1}{1 + e^{\beta(E_X + \mu_N)}},$$

and $E_X = \sqrt{\mathbf{p}^2 + m_X^2}$, $\mu_N = \mu_B - g_\omega \omega$, with $\gamma_N = 2 \times 2$ being the spin-isospin degeneracy factor. We minimize the potential with respect to σ, χ and ω

$$\frac{\partial \Omega}{\partial \sigma} = -\lambda_\chi \chi^2 \sigma + \lambda \sigma^3 - \epsilon \chi^2 + \sum_{X=N_\pm} \frac{\partial m_X}{\partial \sigma} s_X = 0, \tag{12}$$

$$\frac{\partial \Omega}{\partial \omega} = -\lambda_\omega \chi^2 \omega + g_\omega \sum_{X=N_\pm} \rho_X = 0, \tag{13}$$

$$\frac{\partial \Omega}{\partial \chi} = -\lambda_\chi \sigma^2 \chi + \frac{\lambda_\chi^2}{\lambda} \chi^3 - 2\epsilon\sigma\chi - \lambda_\omega \chi \omega^2 + B \frac{\chi^3}{\chi_0^4} \log\left(\frac{\chi}{\chi_0}\right)^4 + \sum_{X=N_\pm} \frac{\partial m_X}{\partial \chi} s_X = 0, \tag{14}$$

where the scalar and the baryon number densities are, respectively,

$$s_X = \gamma_N \int \frac{d^3p}{(2\pi)^3} \frac{m_X}{E_X} (f_X + \bar{f}_X), \tag{15}$$

and

$$\rho_X = \gamma_N \int \frac{d^3p}{(2\pi)^3} (f_X - \bar{f}_X). \tag{16}$$

As mentioned above, with the present parametrization, the contribution of the dilaton field to the ground state properties is numerically negligible. One can check whether χ can influence the nuclear matter equation of state at all. In principle, this is possible but with a lower dilaton mass; see [43]. With a mass of $m_\chi = 1700$ MeV used in this work, the impact of a dilaton field, e.g. on chiral restoration, is expected only at much higher densities. We briefly discuss this possibility in Sec. V.

III. QUARK SECTOR: LINEAR SIGMA MODEL AND STATISTICAL CONFINEMENT

We introduce the quark-meson (QM) coupling according to the linear sigma model

$$\mathcal{L}_q = i\bar{q}\partial\!\!\!/ q + g_q \bar{q}(\sigma + i\gamma_5 \boldsymbol{\tau} \cdot \boldsymbol{\pi}) q - V_\sigma, \tag{17}$$

with the *same* parameters in the σ potential as in Eq. (5) where we considered nuclear matter. For the quark-meson coupling we use $g_q = 300\ \text{MeV}/f_\pi$. The dilaton is too heavy and hence not essential for the following discussion, so we set $\chi = \chi_0$ by hand. The thermodynamics of this model was studied in Refs. [44–46].

A. Shallow potential and early onset of quarks

Using the same model parameters (i.e. low m_σ) that are constrained in Sec. II to obtain reasonable nuclear matter properties gives a shallow potential in the σ direction. A shallow potential leads to a chiral phase transition in cold quark matter at rather low densities, even below n_0 [45]. The corresponding equation of state has a zero-pressure point where quark matter has a finite density. This is illustrated by the red line in Fig. 1 where we plot the density of quarks ρ_q as a function of the quark chemical potential $\mu_q = \mu_B/3$. In our present model we obtain $3\mu_q \simeq 750$ MeV which is lower than the nucleon mass.

This is a striking problem: quarks appear too early due to a shallow potential. A common way to solve this problem is to adjust the chiral potential in the quark sector independently of the nucleonic sector. Such a treatment is not possible in a unified description of nucleon and quark matter. Also, note that a larger m_σ is not favored in view of a nuclear matter ground state. For example, with typical values in quark models $m_\sigma \gtrsim 600$ MeV, compressibility of nuclear matter at saturation increases by an order of magnitude from its experimentally suggested range [21]. In Ref. [14] the problem of a flat potential was circumvented by assigning a bare mass term of 200 MeV to the quarks. We conclude that the essential missing physics is confinement of quarks in the infrared region where their interaction becomes strong. To avoid this inconsistency below we introduce a simple model of *statistical confinement*.

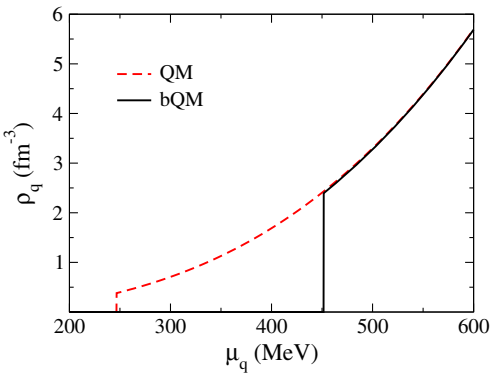

FIG. 1 (color online). Quark number density in the QM and in the bQM model.

B. Statistical confinement of quarks

The concept of statistical confinement is very successful at finite temperatures where the Polyakov loop is used to modify the quark distribution functions [5]. At finite density and small temperature the center symmetry is badly broken so we cannot use the Polyakov loop. As an alternative, we propose a modification of the quark distribution functions via the following ansatz:

$$n_q = \theta(\mathbf{p}^2 - b^2) f_q, \qquad \bar{n}_q = \theta(\mathbf{p}^2 - b^2)\bar{f}_q, \tag{18}$$

where b is a parameter, and f_q and $\bar{f}_q$ are

$$f_q = \frac{1}{1 + e^{\beta(E_q - \mu_q)}}, \qquad \bar{f}_q = \frac{1}{1 + e^{\beta(E_q + \mu_q)}},$$

the Fermi-Dirac distribution functions for quarks and antiquarks, respectively. Obviously, in Eq. (18) quarks with momenta $\mathbf{p}^2 < b^2$ are suppressed.

This is one possible way to restrict thermal quark fluctuations at low momenta. It is similar to the concept of infrared confinement used in the Dyson-Schwinger vacuum studies [47,48] and in the NJL model [31,49–51]. The infrared cutoff is in line with the idea of in-hadron condensates [52], and is also implemented in the holographic hard wall [53] and soft wall [54] models. Intuitively, $1/b$ can be understood as a typical size of a hadron, so that due to the uncertainty principle quarks cannot have momenta lower than b.

With a sharp cutoff in the distribution function it is not possible to saturate the Stefan-Boltzmann limit at high temperature and/or density. Essentially, b must be a medium dependent quantity. A thermodynamically consistent way to achieve this is to promote b to a field generated by some potential V_b. The minimization of the thermodynamic potential in the b direction results in b being a medium dependent quantity. Since the potential V_b is an additional contribution to the bag pressure, this prescription can be understood as a self-consistent way to generate a medium-dependent bag pressure. We therefore name this model the bag-quark-meson model (bQM), and the field b is named the *bag* field. We consider the bag field as a nondynamical, auxiliary field. This field is responsible for statistical confinement, in spirit similar to the Polyakov loop.

Taking into account the modification of the distribution functions, and the vacuum potential V_b, the thermodynamic potential of the model becomes

$$\Omega = V_\sigma + V_b + \Omega_q, \tag{19}$$

where

$$\Omega_q = \gamma_q \int \frac{d^3p}{(2\pi)^3}[T\log(1 - n_q) + T\log(1 - \bar{n}_q)], \tag{20}$$

with n_q given by (18) and $\gamma_q = 2 \times N_f \times N_c = 12$ for two flavors. The gap equations are

$$\frac{\partial\Omega}{\partial\sigma} = -\lambda_\chi \chi_0^2 \sigma + \lambda\sigma^3 - \epsilon\chi_0^2 + g_q s_q = 0, \tag{21}$$

and

$$\frac{\partial\Omega}{\partial b} = \frac{\partial V_b}{\partial b} - \varpi_q = 0, \tag{22}$$

where

$$s_q = \gamma_q \int \frac{d^3p}{(2\pi)^3}\frac{m_q}{E_q}(n_q + n_{\bar{q}}). \tag{23}$$

The term ϖ_q is a boundary contribution of (20)

$$\varpi_q = \gamma_q \frac{b^2}{2\pi^2}[T\log(1 - f_q) + T\log(1 - \bar{f}_q)]_{\mathbf{p}^2 = b^2}. \tag{24}$$

The goal is to suppress quarks at low T and/or μ_q with a large value for b, and to have lower values of b at high T and/or μ_q. Remarkably, this is accomplished through the minimization of the thermodynamic potential with respect to b: the thermal correction ϖ_q to the gap equation for b acts to *reduce* b.

C. Parametrization of the bQM model

Unlike the Polyakov loop potential, the potential V_b cannot be constrained by symmetry, so one should try different forms. Below we consider a special case with a minimal number of terms that yields a finite value of b in the vacuum. Namely, we choose

$$V_b = -\frac{\kappa_b^2}{2}b^2 + \frac{\lambda_b}{4}b^4, \tag{25}$$

where the new parameters κ_b and λ_b must be determined. The nontrivial vacuum expectation value of this potential is $b_0 = \sqrt{\kappa_b^2/\lambda_b}$. One can further motivate this choice as follows. Since the b field generates statistical confinement in our model, we associate it with the chromoelectric part of the gluon sector. The essential reason for this is that finite T lattice computations show that the chromoelectric part of the gluon condensate drops across the pseudocritical temperature [55–57]. Also, the chromoelectric sector is governed by the zeroth component of the gluon fields, like the Polyakov loop or the quark-antiquark potential, so it is essentially nondynamical. In that sense, such an identification can be considered natural.

Since the b potential (25) yields an additional contribution to the vacuum energy, we must ensure that the total vacuum energy remains correctly saturated. We will consider a particular case where the vacuum energy created by the χ field and the b field are equal in magnitude $V_{\chi_0} = V_{b_0}$,

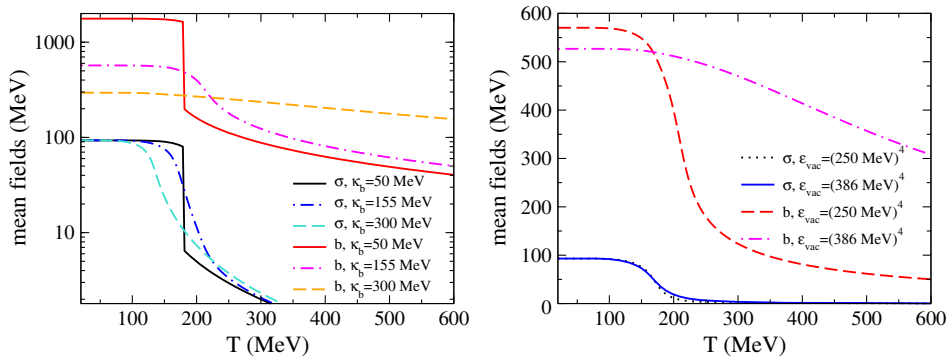

FIG. 2 (color online). The mean fields σ and b in the bQM model as a function of T at $\mu_q = 0$. Left: results for different values of the parameter κ_b, with $\epsilon_{\rm vac} = (250\ {\rm MeV})^4$. Right: results for $\epsilon_{\rm vac} = (250\ {\rm MeV})^4$, $\kappa_b = 155$ MeV and $\epsilon_{\rm vac} = (386\ {\rm MeV})^4$, $\kappa_b = 400$ MeV. In this case, the pseudocritical temperature of the chiral transition is fixed to $T_c = 170$ MeV.

so that half of the total vacuum energy has its origin in the chromoelectric sector [58,59], modeled here by V_b. In this language, the dilaton χ naturally represents the chromomagnetic component of the gluon condensate [26,27,58,59], which survives the chiral transition. We thus take

$$-V_{b_0} = \frac{\kappa_b^4}{4\lambda_b} = \frac{\epsilon_{\rm vac}}{2}, \tag{26}$$

where the total vacuum energy is $\epsilon_{\rm vac} \simeq (193 - 386\ {\rm MeV})^4$. We fixed a value for V_{b_0} (within the range for $\epsilon_{\rm vac}$) and then changed κ_b. We found that, in general, low values of $\epsilon_{\rm vac}$ and low values of κ_b produce a first order chiral transition in the bQM model at $\mu_q = 0$ and finite T; see the left panel of Fig. 2 for $\kappa_b = 50$ MeV. Since lattice QCD shows that the chiral transition is a crossover, this sets a lower bound on κ_b. Increasing κ_b while holding $\epsilon_{\rm vac}$ fixed leads to a decrease of b_0. The result is that the chiral transition turns into a crossover with its onset shifted towards lower temperatures as shown in the left panel of Fig. 2.

As a second constraint, we choose the pseudocritical temperature T_c as obtained in lattice QCD simulations. For $N_f = 2 + 1$ with physical quark masses the Wuppertal-Budapest Collaboration obtained $T_c = 147(2)(3)$ MeV [60], while the HotQCD Collaboration quoted $T_c = 154(9)$ MeV [61]. Since in this paper we work with $N_f = 2$ we will use a slightly larger value $T_c \simeq 170$ MeV [33,34]. This gives $\epsilon_{\rm vac} = (250\ {\rm MeV})^4$ and $\kappa_b = 155$ MeV. From (26) we find $\lambda_b = 0.074$. The resulting σ and b mean fields obtained by solving (21) and (22) at finite T and $\mu_q = 0$ are shown in Fig. 2, where $b_0 = 570.3$ MeV.

With the appropriate modification of the quark number density

$$\rho_q = -\frac{\partial \Omega_q}{\partial \mu_q} = \gamma_q \int \frac{d^3p}{(2\pi)^3}(n_q - \bar{n}_q), \tag{27}$$

we find that the onset of quarks for $\epsilon_{\rm vac} = (250\ {\rm MeV})^4$ in the bQM model at $T = 0$ is at $\mu_q \simeq 450$ MeV. This numerical value must be contrasted to the one in the QM model, where $\mu_q \simeq 250$ MeV.

It must be stressed that the obtained parameters κ_b and λ_b are not unique. The uncertainty in the QCD vacuum energy provides a range for the parameters κ_b and λ_b. The fixed value of the vacuum energy $\epsilon_{\rm vac} = (250\ {\rm MeV})^4$ is the *smallest* value which still satisfies the above-mentioned constraints. Taking higher values of $\epsilon_{\rm vac}$, while keeping T_c fixed we find that both κ_b and λ_b increase. Interestingly, the vacuum expectation value $b_0 = \sqrt{\kappa_b^2/\lambda_b}$ shows a reduction of less than 10% in the range $\epsilon_{\rm vac} = (250 - 386\ {\rm MeV})^4$. The sensitivity to $\epsilon_{\rm vac}$ is reflected in the temperature at which the b field experiences a rapid change. Higher values of $\epsilon_{\rm vac}$ represent a larger energy barrier for quark fluctuations so a delayed and more gradual change in the b field is expected. This is visible in the right panel of Fig. 2 where the b field is shown for $\epsilon_{\rm vac} = (250\ {\rm MeV})^4$ and $\epsilon_{\rm vac} = (386\ {\rm MeV})^4$.

D. Similarities and differences between the bQM and the PQM model

Since a finite b field reduces the strength of the quark thermal fluctuations, it is intuitively clear that it will act to increase the critical temperature associated with the chiral transition (see also left panel of Fig. 2). In the chiral limit we can show this relation analytically by finding a zero of the σ^2 coefficient in the Landau expansion of the thermodynamic potential (19) in powers of σ^2. The result can be cast in the following parametric form:

$$-\lambda_\chi \chi_0^2 + \gamma_q g^2 \frac{T^2}{12}\mathcal{F}\left(\frac{b}{T}\right) = 0, \tag{28}$$

where

$$\mathcal{F}(x) = \frac{2}{\pi^2}(-3x^2 + \pi^2 + 6x\log(1+e^x)) + \frac{12}{\pi^2}\mathrm{Li}_2(-e^x), \tag{29}$$

and $\mathrm{Li}_2(x)$ is the polylogarithm of order 2. In the limit $b/T \ll 1$ this can be simplified to

$$T_c^{\mathrm{bQM}} \simeq \left(\frac{12\lambda_\chi\chi_0^2}{\gamma_q g^2} + \frac{3}{\pi^2}b^2\right)^{1/2}. \tag{30}$$

The second term under the square root is a correction to the usual QM model result for T_c. It is instructive to compare this result to the one obtained in the Polyakov-quark-meson (PQM) model

$$T_c^{\mathrm{PQM}} = \left(\frac{12\lambda_\chi\chi_0^2}{\gamma_q g^2} + \frac{2}{\pi^2}\phi^2\right)^{1/2}, \tag{31}$$

where ϕ is the background gauge field related to the Polyakov loop Φ through $\Phi = [1 + 2\cos(\phi/T)]/3$, see e.g. [5].

In the PQM model the Polyakov loop potential saturates the transverse (physical) gluon contribution to the thermodynamics. On the other hand, in the bQM model the potential V_b does not contain the transverse gluons. This is the main difference between the PQM and the bQM models. In the PQM model, deconfinement transition can be characterized by the Polyakov loop. Then, one can define the pseudocritical temperatures governed by the peaks of the quark condensate and the Polyakov loop and interpret their approximate coincidence as obtained in lattice QCD simulations [60]. However, the bQM model in its present form cannot predict the deconfinement transition temperature, nor the coincidence of the two respective pseudocritical temperatures, because the b field is not a confinement-deconfinement order parameter.

To compare results for the bQM and the PQM models, we have calculated the σ field and the Polyakov loop in a PQM model. A concrete parametrization of the Polyakov loop potential is taken from [62], while for the quark sector the same linear sigma model (17) is used. In Fig. 3 we compare our results where ϵ_{vac} in the bQM model was set to $\epsilon_{\mathrm{vac}} = (250\ \mathrm{MeV})^4$. We find that the σ field in both models are closely matched, with peaks in $d\sigma/dT$ at 163 and 170 MeV (the fitted value), respectively. Obviously, a more realistic consideration should include explicitly the bosonic excitations.

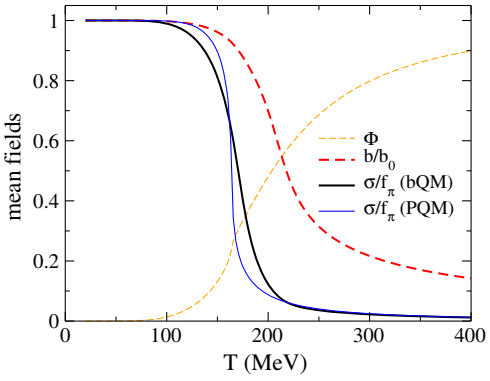

FIG. 3 (color online). A comparison between the normalized mean fields in the bQM and the PQM models as functions of T at $\mu_q = 0$. The bQM results are presented for $\epsilon_{\mathrm{vac}} = (250\ \mathrm{MeV})^4$.

IV. A COMBINED QUARK-MESON-NUCLEON MODEL

In this section we construct a combined quark-meson-nucleon (QMN) model. Our guiding requirement is to exclude quarks at low density, and to exclude nucleons at high density. In the previous section we introduced the concept of statistical confinement of quarks, and now we propose a similar but opposite modification of the distribution functions for nucleons

$$n_{N_\pm} = \theta(\alpha^2 b^2 - \mathbf{p}^2) f_{N_\pm}, \qquad \bar{n}_{N_\pm} = \theta(\alpha^2 b^2 - \mathbf{p}^2)\bar{f}_{N_\pm}. \tag{32}$$

With this ansatz nucleon fluctuations with momenta $\mathbf{p}^2 > (\alpha b)^2$ are suppressed, where α is a new parameter of the model. A similar form has been used in [32]. In Sec. IV B we will determine the possible range for the parameter α.

A. Model setup

The thermodynamic potential of the QMN model is obtained as the following sum:

$$\Omega = V_\sigma + V_\omega + V_\chi + V_b + \sum_{X=N_\pm,q} \Omega_X, \tag{33}$$

with $\Omega_{N_\pm}$ defined as in (11) with the appropriate modification of the distribution functions $f_{N_\pm} \to n_{N_\pm}$ according to Eq. (32), while Ω_q is defined in (20).

The gap equations are obtained by minimizing the thermodynamical potential (33). The ω and χ gap equations remain unchanged by the inclusion of quarks, being given by Eqs. (13) and (14), respectively, and the proper replacement $f_{N_\pm} \to n_{N_\pm}$ according to Eq. (32). The gap equations for σ and b are modified as follows:

$$\frac{\partial\Omega}{\partial\sigma} = -\lambda_\chi\chi^2\sigma + \lambda\sigma^3 - \epsilon\chi^2 + \sum_{X=N_\pm,q}\frac{\partial m_X}{\partial\sigma}s_X = 0, \tag{34}$$

$$\frac{\partial\Omega}{\partial b} = -\kappa_b^2 b + \lambda_b b^3 + \alpha\sum_{X=N_\pm}\varpi_X - \varpi_q = 0, \tag{35}$$

where

TABLE I. The parameters of the quark-meson-nucleon model.

m_σ (MeV)	m_χ (MeV)	B (MeV)^4	g_1	g_2	g_χ	g_ω	g_q	λ	λ_χ	κ_b (MeV)	λ_b
370.63	1700	297.30	13.0	6.97	4.39	6.79	3.22	6.84	3.71	155	0.074

$$\varpi_{N_\pm} = \gamma_N \frac{(\alpha b)^2}{2\pi^2}[T\log(1-f_{N_\pm}) + T\log(1-\bar{f}_{N_\pm})]_{\mathbf{p}^2=(\alpha b)^2}, \tag{36}$$

and ϖ_q is given in (24).

The pressure is calculated by evaluating the thermodynamic potential at its minimum $p = -\Omega + \Omega_0$, normalized with the constant Ω_0 in such a way that the physical vacuum has zero pressure. The total baryon number density is

$$\rho_B = -\frac{\partial\Omega}{\partial\mu_B} = \rho_{N_+} + \rho_{N_-} + \frac{1}{3}\rho_q,$$

where we used $\mu_q = \mu_B/3$. The nucleon and quark particle fractions are defined as

$$Y_{N_\pm} = \frac{\rho_{N_\pm}}{\rho_B}, \qquad Y_q = \frac{1}{3}\frac{\rho_q}{\rho_B}. \tag{37}$$

For the transition from nucleon to quark degrees of freedom the gap equation for the b field, Eq. (35), is crucial. Note that, as a consequence of the Leibniz rule, the nucleon and quark contributions in (35) have opposite signs. In the low density phase nucleons will favor finite b and as a consequence quarks are suppressed. The appearance of quarks at high densities acts to *reduce* b and therefore exclude nucleons. Therefore, Eq. (35) controls the relative abundance of nucleons and quarks. In order to better illustrate this point we have solved a simplified model with only the b field in the Appendix.

B. Parametrization

The parameters of the vacuum potential (as well as the effective masses m_X and chemical potentials μ_X) are defined in Secs. II and III, and collected in Table I. In particular, we will use V_b with $\epsilon_{\rm vac} = (250\ {\rm MeV})^4$ as discussed in Sec. III C. The remaining parameter α is chosen so that the effective UV cutoff αb_0 for the nucleon distribution functions does not spoil the nuclear matter ground state. This sets the minimal value for $\alpha b_0 \gtrsim 300$ MeV. Assume now that at some μ_B there is a transition to quark matter. From the following consideration this will lead to a useful estimate on the upper bound on α. Consider Eq. (35) in the limit of large μ_B. At $T \to 0$ the boundary terms read

$$\varpi_{N_\pm} \to -\gamma_N \frac{(\alpha b)^2}{2\pi^2}(\mu_N - E_{N_\pm})\theta(\mu_N - E_{N_\pm}), \tag{38}$$

$$\varpi_q \to -\gamma_q \frac{b^2}{2\pi^2}(\mu_q - E_q)\theta(\mu_q - E_q). \tag{39}$$

We assume $\sigma, \omega \to 0$ in this limit. In addition, we consider a case where μ_B is large enough that we can also ignore the chirally invariant nucleon mass. Using (38), Eq. (22) simplifies to

$$\frac{\partial\Omega}{\partial b} = -\kappa_b^2 b + \lambda_b b^3 + \frac{b^2}{2\pi^2}\left(-2\alpha^3\gamma_N + \frac{\gamma_q}{3}\right)\mu_B = 0. \tag{40}$$

Since $\gamma_N = \gamma_q/3$, the vanishing bracket defines $\alpha_{\rm max} = 2^{-1/3}$. For $b_0 = 570.3$ MeV we have $\alpha_{\rm max} b_0 = 452.6$ MeV. In the following results we consider two values of the α parameter: $\alpha b_0 = 300$ MeV and $\alpha b_0 = 440$ MeV, which is close to the benchmark value $\alpha_{\rm max} b_0 = 452.6$ MeV. We also calculate the transition points for several α's in between.

V. RESULTS

Without the modification of the nuclear distribution functions the parity doublet model with dilaton introduced in Sec. II has a weak first order chiral transition at $\mu_B \simeq 2110$ MeV for the parameters used here. This should be contrasted to the value of $\mu_B \simeq 1725$ MeV found for the same parameter set [21,22] but using a model without the dilaton. Such a delay in the chiral transition takes place because the dilaton field is essentially coupled to the density through the ω field; see Eq. (6). In the case where the distribution functions are modified we must deal with the uncertainty in the parameter α and $\epsilon_{\rm vac}$. We show explicit calculations for the case $\epsilon_{\rm vac} = (250\ {\rm MeV})^4$ and for two limiting values of α. Finally, we will discuss sensitivity to the uncertainty in $\epsilon_{\rm vac}$.

With $\alpha b_0 = 300$ MeV the onset of chiral-symmetric phase occurs at a lower μ_B. This can be seen on Fig. 4 showing the solutions of the gap equations in the QMN model. This is easily understood: in this model it is the nucleons that restore the chiral symmetry—quarks appear only at higher μ_B; see Fig. 1. The cutoff in the nucleon momenta limits their density, and the ω field reaches a plateau after $\mu_B \simeq 1000$ MeV. Therefore, the shift of μ_B due to the ω field is diminished and, as a consequence, the chiral transition happens at lower μ_B than in the model without a cutoff. At $\alpha b_0 = 300$ MeV the chiral transition is first order and occurs at $\mu_B = 1135$ MeV. After this point, the σ field drops almost to zero and the parity-doublet partners become degenerate and equally populated. In the case $\alpha b_0 = 440$ MeV, the chiral phase transition is a

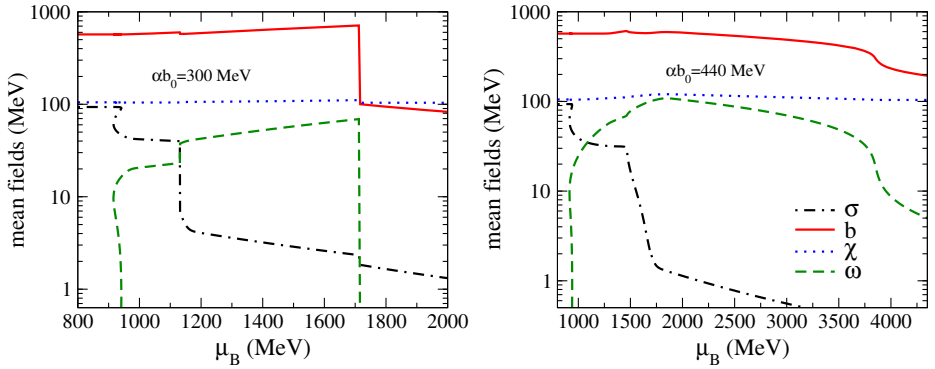

FIG. 4 (color online). The mean fields for the QMN model for two different values of the α parameter indicated in the figure. As μ_B is increased there is a clear imprint of the liquid-gas and the chiral phase transitions on the σ field shown by the dash-dot black line. The drop in the b field at high μ_B is associated with the deconfinement transition.

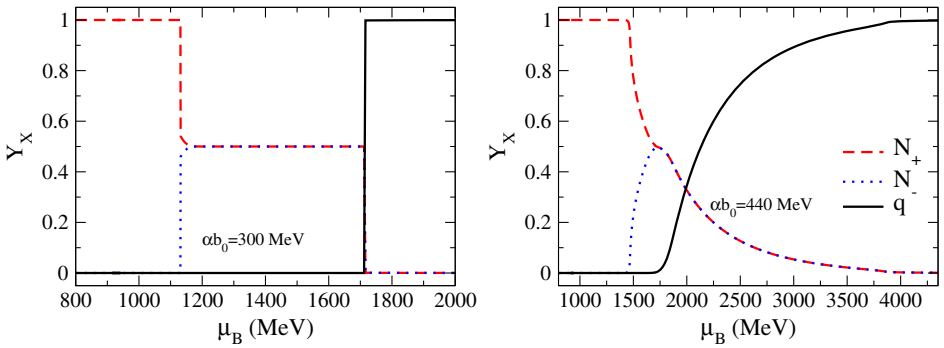

FIG. 5 (color online). Quark and nucleon particle fractions for the QMN model for two different values of the α parameter as indicated in the figure.

crossover. From the peak in $d\sigma/d\mu_B$ we extract $\mu_B = 1473$ MeV. At that point the mass splitting of the parity partners is around 18% of its chirally invariant contribution in the vacuum given by $g_\chi \chi_0 = 790$ MeV.

At some higher μ_B the b field decreases, as can be seen in Fig. 4. The reduction of the b field suppresses nucleons simultaneously enhancing quark fluctuations, according to Eqs. (32) and (18), respectively. Therefore, this marks the deconfinement transition in the QMN model. This is demonstrated in Fig. 5 where we plot the nucleon and quark particle fractions defined in Eq. (37).

The strength of the transitions strongly depends on the value of α. For $\alpha b_0 = 300$ MeV the deconfinement transition is accompanied by a jump in the b field—consequently the baryon density has a jump, so it is rightful to consider this as a first order phase transition. On the other hand, for $\alpha b_0 = 440$ MeV, the b field reduces gradually so that the deconfinement transition is in fact a crossover, allowing for a wide region of a mixed phase of nucleons and quarks; see Fig. 5. In this case we conventionally mark the point of the deconfinement transition with μ_B at which $Y_q = Y_{N_\pm}$ holds. The model predicts that the deconfinement transition happens at $\mu_B^{\rm d} = 1716$ MeV for the case $\alpha b_0 = 300$ MeV, while it occurs at $\mu_B^{\rm d} = 2130$ MeV for $\alpha b_0 = 440$ MeV. The difference between these two cases is seen for example in the behavior of particle fractions in Fig. 5.

The chiral and the deconfinement transition are reflected in the behavior of the density n_B as a function of μ_B, plotted in Fig. 6, and the equation of state, plotted in Fig. 7 in the

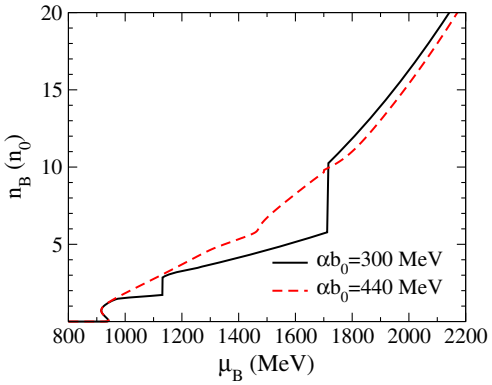

FIG. 6 (color online). The baryon number density n_B (in units of saturation density n_0) as a function of the baryon chemical potential μ_B in the QMN model and for two different values of the α parameter indicated in the figure.

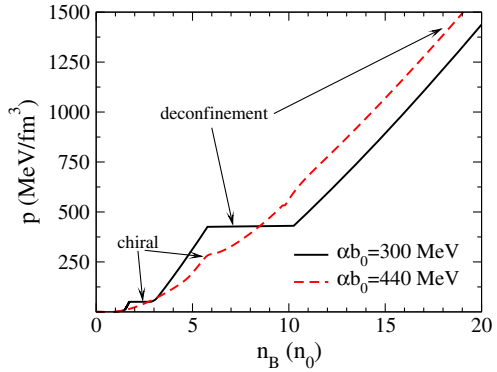

FIG. 7 (color online). The equation of state for the QMN model for two different values of the α parameter indicated in the figure. The locations of the chiral and the deconfinement transition are approximately marked. In the case of $\alpha b_0 = 440$ MeV, the arrow marks the point where $Y_{N_+} + Y_{N_-} = Y_q$.

$p - n_B$ plane. While for both values of α the chiral transition is visible as a small density change, for $\alpha b_0 = 300$ MeV the deconfinement transition has a pronounced density jump in the region $n_B \simeq 6 - 10 n_0$. On the other hand, with $\alpha b_0 = 440$ MeV the deconfinement transition is continuous and there is no clear imprint on the equation of state.

In Table II we collect the numerical values for the chemical potential and the total baryon density at the onset of the chiral and the deconfinement phase transition for several values of α. With increasing α, both the chiral and the deconfinement transition are shifted to higher μ_B. The onset of the chiral phase transition is limited by the value $\mu_B \simeq 2100$ MeV, which is the result for any $\alpha > \alpha_{\max}$. On the other hand, the deconfinement phase transition will be pushed to $\mu_B \to \infty$ as $\alpha \simeq \alpha_{\max}$ is approached. Beyond $\alpha_{\max}$ there is no deconfinement transition. To summarize, we have found that the chiral and the deconfinement transitions in the model do not coincide for any choice of α.

TABLE II. The baryon chemical potential μ_B and the baryon number density n_B at the onset of chiral and the deconfinement phase transitions for several values of α in the QMN model. We also denote the order of the chiral and the deconfinement transition for both cases. In the case of a first order transition, the transition μ_B is defined as a lower value of the number density jump. In the case of a crossover, $\mu_B^{\rm ch}$ is defined by the peak in $d\sigma/d\mu_B$, while $\mu_B^{\rm d}$ is defined as the point where $Y_{N_+} + Y_{N_-} = Y_q$. The values of n_B are given in units of the saturation density $n_0 = 0.16$ fm^{-3}.

αb_0 (MeV)	$\mu_B^{\rm ch}$ (MeV)	$n_B^{\rm ch}$ (n_0)	order	$\mu_B^{\rm d}$ (MeV)	$n_B^{\rm d}$ (n_0)	order
300	1132	1.7	First	1716	5.8	First
350	1220	2.8	First	1851	9.0	First
400	1348	4.4	Crossover	1931	11.7	First
440	1473	6.1	Crossover	2130	18.1	Crossover

Lattice QCD results predict that the chiral and the confinement transitions approximately coincide along the finite T axes of the QCD phase diagram. We have performed calculations at two nonzero temperatures, $T = 50$ MeV and $T = 100$ MeV to test whether such a tendency may be observed within the QMN model. At $T = 0$ MeV the separation between the two transitions is roughly $\Delta\mu_B \sim 580 - 660$ MeV (see Table II), within the explored α range. With $T = 50$ MeV we find $\Delta\mu_B \sim 560 - 880$ while at $T = 100$ MeV we find $\Delta\mu_B \sim 420 - 850$ MeV, i.e. there is no clear trend in the critical parameter.

Taking into account the uncertainty in $\epsilon_{\rm vac} = (250 - 386\ {\rm MeV})^4$ does not lead to a significant modification in the above results. We have explicitly checked that for $\epsilon_{\rm vac} = (386\ {\rm MeV})^4$ the b field changes more gradually with increasing μ_B (similar to the finite T results presented in Fig. 2) thereby softening the chiral and the deconfinement transition.

VI. CONCLUSIONS

The properties of matter at large baryon densities are almost exclusively considered either in purely nucleonic models, or within purely quark models, with rare attempts at a unified description [14,32,63–65]. A crucial ingredient for a unified description should be an effective mechanism to exclude quarks in the dilute hadronic matter, and to exclude nucleons at asymptotically high densities. While the former has been accomplished by coupling quarks to the Polyakov loop, it is applicable only at finite temperatures and low densities. In this work we have used a simplistic modification of the distribution functions of both the nucleons and the quarks that provides a mechanism to exclude quarks at low density and nucleons at high density.

We have considered nuclear matter in a parity doublet model with mirror assignment coupled to the dilaton field. We have argued that the chiral potential which is fitted to the nuclear ground state properties is shallow (i.e. the σ meson is light). When the same potential is used for quark matter it yields an early onset of quarks. This is especially acute at zero temperature, where we find that with such a chiral potential the onset of quarks happens at baryon chemical potential below the nucleon mass. Chiral models of nuclear matter usually favor low m_σ, see e. g. [21,66–68], so the problem of the shallow potential seems to be somewhat general. However, we stress that it is a problem only if we choose to couple the quarks to the same σ field.

We have proposed a possible solution of this problem by introducing the concept of statistical confinement for quarks. The quark distribution functions were modified in such a way that the quarks are suppressed below some particular momentum. We associate this minimum momentum with an auxiliary scalar field, named the bag field. This field brings a new contribution to the total vacuum potential. We have found that the minimization of the

thermodynamic potential in the b direction provides a thermodynamically consistent framework. Moreover, the b field is finite in the vacuum and is reduced as temperature or density is increased. At finite temperatures the mechanism of suppression of quarks is similar to the effect of the Polyakov loop. We have proposed a phenomenological form for the bag potential and fitted its parameters to the QCD vacuum energy $\epsilon_{\rm vac}$ and to T_c at $\mu_B = 0$ known from the lattice simulations. Within this scheme it was possible to solve the problem of a shallow potential.

Further on, we have generalized the nucleonic distribution functions, by restricting their ultraviolet momentum space up to a value αb where α is an additional parameter in the model. We have used the same bag potential to construct a combined quark-meson-nucleon model. The vital feature of this model is that both the quarks and the nucleons are coupled to the same bosonic fields. Then the fate of the QCD phase transitions was investigated at finite densities.

We explored a range of values for the parameter α and found that an increase in α delays the onset of the chiral and the deconfinement transitions. The requirements that the nuclear ground state is not affected by quarks, and that the deconfinement transition happens at some density, restrict α to a finite range. Taking into account the uncertainty in $\epsilon_{\rm vac}$ within this range of α we find that the chiral transition occurs at $\mu_B^{\rm ch} \simeq 1100 - 2100$ MeV. For the deconfinement transition we predict a lower bound $\mu_B^{\rm d} \gtrsim 1700$ MeV. In terms of the density the corresponding values are $n_B^{\rm ch} \simeq 1.5 - 15.5 n_0$ and $n_B^{\rm d} \gtrsim 5 n_0$. For the lowest value $\epsilon_{\rm vac} = (250\ {\rm MeV})^4$ order of both phase transitions depends on the value of particular α. With low values of α both transitions are first order, while for the higher values of α they are smooth crossovers. Especially, the deconfinement transition proceeds in a broad crossover mixed phase where nucleons and quarks coexist. These features persist as we vary $\epsilon_{\rm vac}$.

In this model the chiral and the deconfinement transition are always separated. The chiral transition is driven by the nucleonic fluctuations for any α. It is suggestive to consider this result in the light of the calculation of the Wilson and the Polyakov loop on the lattice with Dirac zero modes artificially removed. In Refs. [69,70] it was found that in this chirally "unbroken" phase the Wilson loop still displays an area law, and that the Polyakov loop is almost zero. The separation of the transitions might be considered as a manifestation of the quarkyonic phase [71,72], where chiral symmetry is restored in the nucleonic phase.[1]

The separation of the chiral and the deconfinement transition persists also at nonzero T, where we checked two values $T = 50$ MeV and $T = 100$ MeV. However, we do not expect the QMN model itself to be valid at such high T where gluons and lightest hadrons become important. Since in the QMN model we cannot calculate the Polyakov loop, the deconfinement transition in this case must be characterized in a different way. For these reasons, the fit of V_b to lattice T_c, performed here only in the very simple bQM model, carries systematic uncertainties. In general, the comparison to lattice QCD should be revised within a more complete approach before addressing the full $T - \mu_B$ phase diagram.

We must emphasize that the bag field should not be considered as an order parameter in this model, since it is not connected to any of the fundamental QCD symmetries. In particular, it must not be considered as an order parameter for the deconfinement transition, even though it does play a key role in establishing it. The value of μ_B where the transition occurs is for some values of the α parameter accompanied by a finite jump in the total baryon density. In these cases, the density contrast between two coexisting phases can be used to characterize the deconfinement phase transition. We can draw an immediate analogy to the liquid-gas phase transition which does not have an order parameter related to a symmetry, but is also characterized by a jump in the density from the liquid to the gas phase.

The approach to the deconfinement transition presented in this work is based on the phenomenological requirements and not rigorously grounded in QCD. Because of this, systematic uncertainties are expected, especially concerning the freedom in choice of the bag potential and the explicit form for the modification of the distribution functions. It would be very interesting to obtain first-principle information about the finite density distribution functions from Dyson-Schwinger studies; see e.g. [73]. This microscopic input could then be used to construct more realistic effective models of nuclear and quark matter.

ACKNOWLEDGMENTS

The visits of S. B. to the Frankfurt Institute of Advanced Studies were supported by the mobility program of the University of Zagreb and by the COST Action MP1304 NewCompStar within the STSM program. S. B. acknowledges partial support by the Croatian Science Foundation under Project No. 8799. The work of I. M. and C. S. was partly supported by the Hessian LOEWE initiative through the Helmholtz International Center for FAIR (HIC for FAIR). I. M. acknowledges partial support from Grant No. NS-932.2014.2 (Russia). C. S. acknowledges partial support by the Polish Science Foundation (NCN) under Maestro Grant No. DEC-2013/10/A/ST2/00106.

APPENDIX

This appendix is devoted to solving a simplified version of the quark-meson-nucleon model, where we focus only on the role of the bag field b. The masses of nucleons and

[1]It is important to stress this does not mean that the nucleons are massless, but that the parity partners are degenerate.

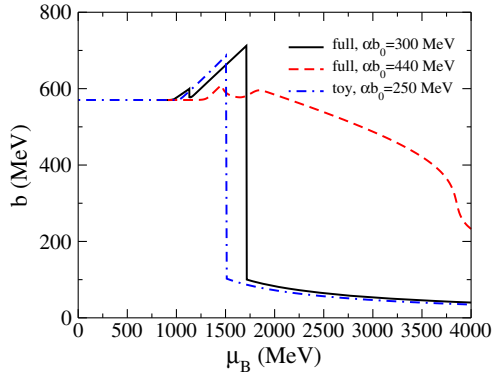

FIG. 8 (color online). The bag field as a function of μ_B in the simplified quark-meson-nucleon model, denoted by the blue, dash-dotted line. For comparison we also plot the bag field from the full quark-meson-nucleon model for two different values of α calculated in Sec. V.

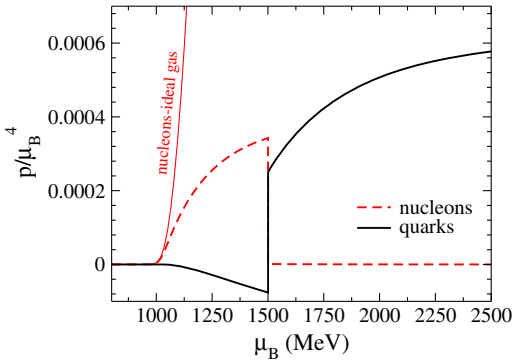

FIG. 9 (color online). Normalized partial pressures of the nucleon and the quark sectors as a function of μ_B in the simplified quark-meson-nucleon model. The ideal nucleon pressure is plotted for comparison.

quarks are held fixed to 1000 and 0 MeV, respectively. With all the other mean fields except the b field discarded, the thermodynamic potential takes the following form:

$$\Omega = V_b + \sum_{X=q,N_\pm} \gamma_X \int \frac{d^3p}{(2\pi)^3} [T\log(1-n_X) + T\log(1-\bar{n}_X)]. \quad \text{(A1)}$$

For the potential V_b we use the same Eq. (25) with the parameters $\kappa_b = 155$ MeV, $\lambda_b = 0.074$. For the parameter α we take the value $\alpha b_0 = 250$ MeV. The partial pressures of quarks (p_q) and nucleons (p_N) are calculated as

$$p_q = -(V_b - V_{b_0}) - \Omega_q, \qquad p_N = -\Omega_{N_+} - \Omega_{N_-},$$

where the pressure contribution arising from V_b is naturally assigned to quarks.

From the minimization of the thermodynamic potential (A1) we obtain b as a function of μ_B shown on Fig. 8. The b field follows its vacuum value up to $\mu_B = 1000$ MeV, then it begins to increase. The increase is due to the fact that nucleons favor a finite value of μ_B according to Eq. (35). We expect the onset of quark degrees of freedom around $\mu_B \simeq 3b_0 \simeq 1700$ MeV. An explicit calculation gives $\mu_B = 1515$ MeV. This point marks the sudden drop of the b field as seen in Fig. 8. The qualitatively similar characteristics are found in Sec. V in the complete model for $\alpha b_0 = 300$ MeV, also shown in Fig. 8. However, for higher $\alpha b_0 = 440$ MeV the transition becomes gradual and shifts to higher μ_B.

In Fig. 9 we plot the partial pressures as a function of μ_B. The nucleon pressure, given by the thick dashed red line, shows significant deviations from its ideal gas formula, shown by a thin red line. In particular, at $\mu_B = 1515$ MeV the nucleon pressure suddenly drops to zero value. The pressure arising from the quarks at first turns to negative values. The reason behind this is the increase of the b field in the region $\mu_B = 1000$–1515 MeV. However, we stress that the total pressure of the system is always non-negative and continuous. After $\mu_B = 1515$ MeV, nucleons disappear and the quark pressure becomes positive. Moreover, since quarks become the dominant degrees of freedom in the system, the value $\mu_B = 1515$ MeV marks the deconfinement transition point for this simplified model.

[1] K. Fukushima and C. Sasaki, The phase diagram of nuclear and quark matter at high baryon density, Prog. Part. Nucl. Phys. **72**, 99 (2013).
[2] N. Brambilla, S. Eidelman, P. Foka, S. Gardner, A. S. Kronfeld, M. G. Alford, R. Alkofer, M. Butenschoen *et al.*, QCD and strongly coupled gauge theories: Challenges and perspectives, Eur. Phys. J. C **74**, 2981 (2014).
[3] M. Buballa, V. Dexheimer, A. Drago, E. Fraga, P. Haensel, I. Mishustin, G. Pagliara, J. Schaffner-Bielich *et al.*, EMMI rapid reaction task force meeting on quark matter in compact stars, J. Phys. G **41**, 123001 (2014).
[4] K. Fukushima, Baryonic matter and beyond, Nucl. Phys. **A931**, 257 (2014).
[5] K. Fukushima, Chiral effective model with the Polyakov loop, Phys. Lett. B **591**, 277 (2004).
[6] C. Ratti, M. A. Thaler, and W. Weise, Phases of QCD: Lattice thermodynamics and a field theoretical model, Phys. Rev. D **73**, 014019 (2006).

[7] S. Roessner, C. Ratti, and W. Weise, Polyakov loop, diquarks and the two-flavor phase diagram, Phys. Rev. D **75**, 034007 (2007).
[8] K. Yamazaki and T. Matsui, Quark-hadron phase transition in the PNJL model for interacting quarks, Nucl. Phys. **A913**, 19 (2013).
[9] A. Wergieluk, D. Blaschke, Y. L. Kalinovsky, and A. Friesen, Pion dissociation and Levinson's theorem in hot PNJL quark matter, Phys. Part. Nucl. Lett. **10**, 660 (2013).
[10] A. Jakovac, Hadron melting and QCD thermodynamics, Phys. Rev. D **88**, 065012 (2013).
[11] K. Yamazaki and T. Matsui, Quark-hadron phase transition in a three flavor PNJL model for interacting quarks, Nucl. Phys. **A922**, 237 (2014).
[12] D. Blaschke, D. Zablocki, M. Buballa, A. Dubinin, and G. Roepke, Generalized Beth–Uhlenbeck approach to mesons and diquarks in hot, dense quark matter, Ann. Phys. (Amsterdam) **348**, 228 (2014).
[13] D. Blaschke, A. Dubinin, and L. Turko, Mott-hadron resonance gas and lattice QCD thermodynamics, arXiv: 1501.00485.
[14] J. Steinheimer, S. Schramm, and H. Stocker, The hadronic SU(3) parity doublet model for dense matter, its extension to quarks and the strange equation of state, Phys. Rev. C **84**, 045208 (2011).
[15] S. Benic, D. Blaschke, D. E. Alvarez-Castillo, T. Fischer, and S. Typel, A new quark-hadron hybrid equation of state for astrophysics—I. High-mass twin compact stars, Astron. Astrophys. **577**, A40 (2015).
[16] V. Dexheimer, R. Negreiros, and S. Schramm, The role of strangeness in hybrid stars and possible observables, Phys. Rev. C **91**, 055808 (2015).
[17] L. M. Satarov, K. A. Bugaev, and I. N. Mishustin, Equation of state and sound velocity of hadronic gas with hard-core interaction, Phys. Rev. C **91**, 055203 (2015).
[18] C. E. Detar and T. Kunihiro, Linear σ model with parity doubling, Phys. Rev. D **39**, 2805 (1989).
[19] T. Hatsuda and M. Prakash, Parity doubling of the nucleon and first order chiral transition in dense matter, Phys. Lett. B **224**, 11 (1989).
[20] D. Jido, Y. Nemoto, M. Oka, and A. Hosaka, Chiral symmetry for positive and negative parity nucleons, Nucl. Phys. **A671**, 471 (2000).
[21] D. Zschiesche, L. Tolos, J. Schaffner-Bielich, and R. D. Pisarski, Cold, dense nuclear matter in a SU(2) parity doublet model, Phys. Rev. C **75**, 055202 (2007).
[22] C. Sasaki and I. Mishustin, Thermodynamics of dense hadronic matter in a parity doublet model, Phys. Rev. C **82**, 035204 (2010).
[23] V. Dexheimer, S. Schramm, and D. Zschiesche, Nuclear matter and neutron stars in a parity doublet model, Phys. Rev. C **77**, 025803 (2008).
[24] S. Gallas, F. Giacosa, and G. Pagliara, Nuclear matter within a dilatation-invariant parity doublet model: The role of the tetraquark at nonzero density, Nucl. Phys. **A872**, 13 (2011).
[25] C. Sasaki, H. K. Lee, W. G. Paeng, and M. Rho, Conformal anomaly and the vector coupling in dense matter, Phys. Rev. D **84**, 034011 (2011).
[26] W. G. Paeng, H. K. Lee, M. Rho, and C. Sasaki, Dilaton-limit fixed point in hidden local symmetric parity doublet model, Phys. Rev. D **85**, 054022 (2012).
[27] W. G. Paeng, H. K. Lee, M. Rho, and C. Sasaki, Interplay between ω-nucleon interaction and nucleon mass in dense baryonic matter, Phys. Rev. D **88**, 105019 (2013).
[28] C. Sasaki and I. Mishustin, The phase structure of a chiral model with dilatons in hot and dense matter, Phys. Rev. C **85**, 025202 (2012).
[29] T. Boeckel and J. Schaffner-Bielich, A little inflation at the cosmological QCD phase transition, Phys. Rev. D **85**, 103506 (2012).
[30] J. Schechter, Effective Lagrangian with two color singlet gluon fields, Phys. Rev. D **21**, 3393 (1980).
[31] D. Ebert, T. Feldmann, and H. Reinhardt, Extended NJL model for light and heavy mesons without $q - \bar{q}$ thresholds, Phys. Lett. B **388**, 154 (1996).
[32] J. Berges, D. U. Jungnickel, and C. Wetterich, Quark and nuclear matter in the linear chiral meson model, Int. J. Mod. Phys. A **18**, 3189 (2003).
[33] S. Ejiri, Lattice QCD at finite temperature, Nucl. Phys. B, Proc. Suppl. **94**, 19 (2001).
[34] Y. Maezawa, S. Aoki, S. Ejiri, T. Hatsuda, N. Ishii, K. Kanaya, and N. Ukita, Thermodynamics of two-flavor lattice QCD with an improved Wilson quark action at non-zero temperature and density, J. Phys. G **34**, S651 (2007).
[35] L. Y. Glozman, C. B. Lang, and M. Schrock, Symmetries of hadrons after unbreaking the chiral symmetry, Phys. Rev. D **86**, 014507 (2012).
[36] G. Aarts, C. Allton, S. Hands, B. Jger, C. Praki, and J. I. Skullerud, Nucleons and parity doubling across the deconfinement transition, arXiv:1502.03603.
[37] J. Sexton, A. Vaccarino, and D. Weingarten, Numerical evidence for the observation of a scalar glueball, Phys. Rev. Lett. **75**, 4563 (1995).
[38] Y. Chen, A. Alexandru, S. J. Dong, T. Draper, I. Horvath, F. X. Lee, K. F. Liu, N. Mathur *et al.*, Glueball spectrum and matrix elements on anisotropic lattices, Phys. Rev. D **73**, 014516 (2006).
[39] M. A. Shifman, A. I. Vainshtein, and V. I. Zakharov, QCD and Resonance Physics. Sum rules, Nucl. Phys. **B147**, 385 (1979).
[40] S. Narison, Gluon Condensates and $m_{c,b}$ from QCD-Moments and their ratios to Order α_s^3 and $\langle G^4 \rangle$, Phys. Lett. B **706**, 412 (2012).
[41] S. Janowski, F. Giacosa, and D. H. Rischke, Is $f_0(1710)$ a glueball?, Phys. Rev. D **90**, 114005 (2014).
[42] C. A. Dominguez, L. A. Hernandez, and K. Schilcher, Determination of the gluon condensate from data in the charm-quark region, arXiv:1411.4500.
[43] P. Papazoglou, J. Schaffner, S. Schramm, D. Zschiesche, H. Stoecker, and W. Greiner, Phase transition in the chiral sigma-omega model with dilatons, Phys. Rev. C **55**, 1499 (1997).
[44] A. Gocksch, Chiral symmetry in hot QCD, Phys. Rev. Lett. **67**, 1701 (1991).
[45] O. Scavenius, A. Mocsy, I. N. Mishustin, and D. H. Rischke, Chiral phase transition within effective models with constituent quarks, Phys. Rev. C **64**, 045202 (2001).

[46] E. S. Bowman and J. I. Kapusta, Critical points in the linear sigma model with quarks, Phys. Rev. C **79**, 015202 (2009).
[47] H. L. L. Roberts, C. D. Roberts, A. Bashir, L. X. Gutierrez-Guerrero, and P. C. Tandy, Abelian anomaly and neutral pion production, Phys. Rev. C **82**, 065202 (2010).
[48] H. L. L. Roberts, A. Bashir, L. X. Gutierrez-Guerrero, C. D. Roberts, and D. J. Wilson, π and ρ mesons, and their diquark partners, from a contact interaction, Phys. Rev. C **83**, 065206 (2011).
[49] W. Bentz and A. W. Thomas, The stability of nuclear matter in the Nambu-Jona-Lasinio model, Nucl. Phys. **A696**, 138 (2001).
[50] D. Blaschke, G. Burau, M. K. Volkov, and V. L. Yudichev, Chiral quark model with infrared cutoff for the description of meson properties in hot matter, Eur. Phys. J. A **11**, 319 (2001).
[51] A. Dubinin, D. Blaschke, and Y. L. Kalinovsky, Pion and sigma meson dissociation in a modified NJL model at finite temperature, Acta Phys. Pol. B Proc. Suppl. **7**, 215 (2014).
[52] S. J. Brodsky and R. Shrock, Maximum wavelength of confined quarks and gluons and properties of quantum chromodynamics, Phys. Lett. B **666**, 95 (2008).
[53] J. Polchinski and M. J. Strassler, Hard Scattering and Gauge/String Duality, Phys. Rev. Lett. **88**, 031601 (2002).
[54] A. Karch, E. Katz, D. T. Son, and M. A. Stephanov, Linear confinement and AdS/QCD, Phys. Rev. D **74**, 015005 (2006).
[55] M. D'Elia, A. Di Giacomo, and E. Meggiolaro, Gauge invariant field strength correlators in pure Yang-Mills and full QCD at finite temperature, Phys. Rev. D **67**, 114504 (2003).
[56] D. E. Miller, Lattice QCD calculation for the physical equation of state, Phys. Rep. **443**, 55 (2007).
[57] P. Colangelo, F. Giannuzzi, S. Nicotri, and F. Zuo, Temperature and chemical potential dependence of the gluon condensate: A holographic study, Phys. Rev. D **88**, 115011 (2013).
[58] H. K. Lee and M. Rho, Dilatons in hidden local symmetry for hadrons in dense matter, Nucl. Phys. **A829**, 76 (2009).
[59] C. Sasaki, I. Mishustin, and K. Redlich, Implementation of chromomagnetic gluons in Yang-Mills thermodynamics, Phys. Rev. D **89**, 014031 (2014).
[60] S. Borsanyi, Z. Fodor, C. Hoelbling, S. D. Katz, S. Krieg, C. Ratti, and K. K. Szabó, Is there still any T_c mystery in lattice QCD? Results with physical masses in the continuum limit III, J. High Energy Phys. 09 (2010) 073.
[61] A. Bazavov, T. Bhattacharya, M. Cheng, C. DeTar, H. T. Ding, S. Gottlieb, R. Gupta, P. Hegde *et al.*, The chiral and deconfinement aspects of the QCD transition, Phys. Rev. D **85**, 054503 (2012).
[62] K. Fukushima, Phase diagrams in the three-flavor Nambu-Jona-Lasinio model with the Polyakov loop, Phys. Rev. D **77**, 114028 (2008); **78**, 039902(E) (2008).
[63] J. Meyer, K. Schwenzer, and H. J. Pirner, Unifying nucleon and quark dynamics at finite baryon number density, Phys. Lett. B **473**, 25 (2000).
[64] S. Lawley, W. Bentz, and A. W. Thomas, Nucleons, nuclear matter and quark matter: A Unified NJL approach, J. Phys. G **32**, 667 (2006).
[65] V. A. Dexheimer and S. Schramm, Novel approach to model hybrid stars, Phys. Rev. C **81**, 045201 (2010).
[66] J. Boguta, A saturating chiral field theory of nuclear matter, Phys. Lett. **120B**, 34 (1983).
[67] P. J. Ellis, E. K. Heide, and S. Rudaz, On scale and chiral symmetry in nuclear matter, Phys. Lett. B **282**, 271 (1992); J. Ellis, S. Kelley, and D. V. Nanopoulos, Constraints from gauge coupling unification on the scale of supersymmetry breaking, Phys. Lett. B **287**, 95 (1992).
[68] I. Mishustin, J. Bondorf, and M. Rho, Chiral symmetry, scale invariance and properties of nuclear matter, Nucl. Phys. **A555**, 215 (1993).
[69] S. Gongyo, T. Iritani, and H. Suganuma, Gauge-invariant formalism with a Dirac-mode expansion for confinement and chiral symmetry breaking, Phys. Rev. D **86**, 034510 (2012).
[70] T. M. Doi, H. Suganuma, and T. Iritani, Relation between confinement and chiral symmetry breaking in temporally odd-number lattice QCD, Phys. Rev. D **90**, 094505 (2014).
[71] Y. Hidaka, L. D. McLerran, and R. D. Pisarski, Baryons and the phase diagram for a large number of colors and flavors, Nucl. Phys. **A808**, 117 (2008).
[72] L. McLerran, K. Redlich, and C. Sasaki, Quarkyonic matter and chiral symmetry breaking, Nucl. Phys. **A824**, 86 (2009).
[73] T. Klahn, C. D. Roberts, L. Chang, H. Chen, and Y. X. Liu, Cold quarks in medium: An equation of state, Phys. Rev. C **82**, 035801 (2010).